



Reaction behavior of ferric oxide in system $\text{Fe}_2\text{O}_3\text{-SiO}_2\text{-Al}_2\text{O}_3$ during reductive sintering process

Qiu-sheng ZHOU, Chuang LI, Xiao-bin LI, Zhi-hong PENG, Gui-hua LIU, Tian-gui QI

School of Metallurgy and Environment, Central South University, Changsha 410083, China

Received 29 April 2015; accepted 11 September 2015

Abstract: Pure compounds and kaolin were employed to investigate the reaction behavior of ferric oxide in the ternary system $\text{Fe}_2\text{O}_3\text{-SiO}_2\text{-Al}_2\text{O}_3$ during reductive sintering process. The thermodynamic analyses and reductive sintering experimental results show that ferrous oxide generated from the reduction of ferric oxide by carbon can react with silicon dioxide and aluminum oxide to form ferrous silicate and hercynite at 1173 K, respectively. In the ternary system $\text{Fe}_2\text{O}_3\text{-SiO}_2\text{-Al}_2\text{O}_3$, ferrous oxide obtained from ferric oxide reduction preferentially reacts with aluminum oxide to form hercynite, and the reaction of ferrous oxide with silicon dioxide occurs only when there is surplus ferrous oxide after the exhaustion of aluminum oxide. When sintering temperature rises to 1473 K, hercynite further reacts with silicon dioxide to form mullite and ferrous oxide. Results presented in this work may throw a new light upon the separation of alumina and silica present in Al/Fe-bearing materials with low mass ratio of alumina to silica in alumina production.

Key words: reductive sintering; ferric oxide; ferrous silicate; hercynite; mullite; kaolin

1 Introduction

Much attention has been paid to the comprehensive recovery and utilization of low grade bauxite [1] as well as secondary aluminum-containing resources such as Bayer red mud and coal ash in China [2,3]. These unmanageable aluminum-bearing resources mainly consist of Al_2O_3 , SiO_2 and Fe_2O_3 [4,5]. Although there are considerable studies on the treatment of these resources, lots of problems still exist. When we extract various valuable metallic elements from them [6–8], the high extraction ratio and the economics cannot be achieved simultaneously. As for secondary aluminum-containing resources, when they are used as environmental functional materials [9–12], the usage and dosage would be restricted due to their complex chemical compositions. For instance, the most studied soda–lime sintering process [13] is an effective method to realize the comprehensive utilization of these resources; however, it has some inherent drawbacks, such as lots of liquid phases formed readily during the sintering process, low recovery of Fe_2O_3 and narrow temperature range for sintering [14]. Therefore, it is

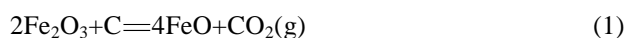
necessary to investigate the reaction behavior of system $\text{Fe}_2\text{O}_3\text{-SiO}_2\text{-Al}_2\text{O}_3$ for exploring novel recovery method, especially the reaction behavior of Fe_2O_3 in the reductive atmosphere as the interreaction can hardly occur except the reactions between SiO_2 and Al_2O_3 in the oxidative atmosphere.

Unfortunately, few researches on the reaction behavior of Fe_2O_3 during reductive sintering process in system $\text{Fe}_2\text{O}_3\text{-SiO}_2\text{-Al}_2\text{O}_3$ have been reported in the literature. KELLEY [15] prepared Fe_2SiO_4 by heating finely powdered silica, ferric oxide and iron mixtures in nickel cartridge placed in an evacuated silica tube at 1040 K for several days. However, the residence time is somewhat long, greatly affecting production efficiency. ZHANG et al [16] reported that hercynite could be synthesized from iron scrap, Fe_2O_3 powder and Al_2O_3 powder by sintering process at 1823 K for 3 h but the hercynite content is only 20% (mass fraction) in the clinker. SCHAIRER [17] studied system $\text{FeO-SiO}_2\text{-Al}_2\text{O}_3$ and presented phase assemblages of system $\text{FeO-SiO}_2\text{-Al}_2\text{O}_3$ at different temperatures, but the generating conditions and formation laws of ferrous silicate, hercynite and mullite were not mentioned. What's more, He could not determine whether the

mullite was synthesized from the reaction of silicon dioxide and aluminum oxide or from the reaction of silicon dioxide and hercynite. In addition, the thermodynamics of system $\text{Fe}_2\text{O}_3\text{-SiO}_2\text{-Al}_2\text{O}_3$ during reductive sintering process was seldom studied in the previous work, which is extremely important for us to study the system experimentally. On the other hand, our preliminary research showed that ferric oxide could react with aluminum oxide to form hercynite which would not further react with silicon dioxide under appropriate reductive sintering conditions. Considering the fact that hercynite is paramagnetic and insoluble in alkaline or acidic solutions [18,19], we could realize the separation of aluminum oxide and silicon dioxide in the aluminosilicates. Under this circumstance, the thermodynamics of reactions among the components in system $\text{Fe}_2\text{O}_3\text{-SiO}_2\text{-Al}_2\text{O}_3$ was firstly studied during reductive sintering process, and then based on the thermodynamics, binary systems $\text{Fe}_2\text{O}_3\text{-SiO}_2$, $\text{Fe}_2\text{O}_3\text{-Al}_2\text{O}_3$ and ternary system $\text{Fe}_2\text{O}_3\text{-SiO}_2\text{-Al}_2\text{O}_3$ during reductive sintering process were studied experimentally using pure compounds as raw materials to reveal the reaction behavior of ferric oxide. Furthermore, the kaolin was employed to verify the experimental results, attempting to throw a new light upon the comprehensive treatment of abovementioned unmanageable aluminum-bearing resources.

2 Thermodynamic analyses of system $\text{Fe}_2\text{O}_3\text{-SiO}_2\text{-Al}_2\text{O}_3$ during reductive sintering process

Carbon powder was employed as reductive agent to study the reductive sintering process of system $\text{Fe}_2\text{O}_3\text{-SiO}_2\text{-Al}_2\text{O}_3$. The main possible reactions involved in this system are listed as follows:



By consulting the practical thermodynamic data manual of inorganic substances [20], Reactions (1)–(4) are analyzed by thermodynamic calculation, and the relationship between Gibbs free energy change and sintering temperature is illustrated in Fig. 1, where quartz, cristobalite and tridymite are three different phases of silicon dioxide in Reactions (3) and (4).

As shown in Fig. 1, the Gibbs free energy change of Reaction (1) decreases with the increase of the temperature and comes to zero at the temperature of about 610 K, meaning that Reaction (1) occurs spontaneously when the temperature is higher than

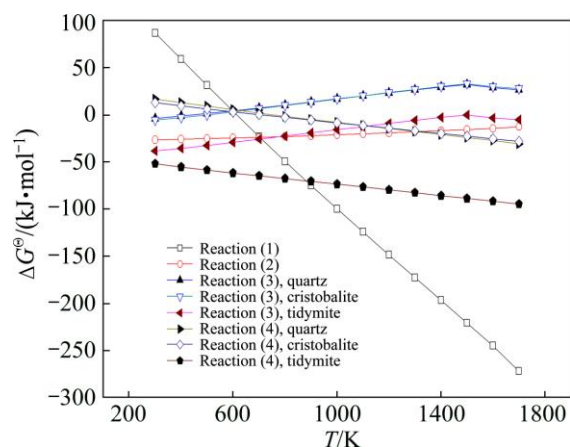


Fig. 1 Relationship between Gibbs free energy changes of Reactions (1)–(4) and sintering temperature

610 K. As for the reaction of ferrous oxide and aluminum oxide (Reaction (2)), the Gibbs free energy change increases slowly as sintering temperature rises, and Reaction (2) can take place to form hercynite at 300–1700 K with the same reaction tendency reported by MEI et al [21] in 1994. In the case of the reaction of ferrous oxide and silicon dioxide (Reaction (3)), the Gibbs free energy change increases with the increase of the temperature in spite of the crystal form of silicon dioxide. The curves corresponding to the reaction of quartz with ferrous oxide and the reaction of cristobalite with ferrous oxide appear to overlap, and the Gibbs free energy changes of these two reactions change from negative to positive at approximately 500 K, illustrating that they would not occur spontaneously at the temperatures higher than 500 K. Tridymite, however, can react with ferrous oxide spontaneously at 300–1700 K and its corresponding curve intersects the curve of Reaction (2) at about 1073 K, indicating that hercynite is more likely to form at the sintering temperature over 1073 K and ferrous silicate forms preferentially at temperatures lower than 1073 K. In regard to the mullite formation reaction (Reaction (4)), the Gibbs free energy change decreases with increasing temperature for different crystal forms of silicon dioxide. The curves corresponding to the reaction of aluminum oxide with quartz and with cristobalite are also essentially overlapped, and the Gibbs free energy changes of these two reactions turn from positive to negative at about 700 K, manifesting that these two reactions may occur at the temperature higher than 700 K. In contrast, aluminum oxide may react with tridymite thermodynamically at 300–1700 K.

Therefore, in system $\text{Fe}_2\text{O}_3\text{-SiO}_2\text{-Al}_2\text{O}_3$ during reductive sintering process with the temperature lower than 610 K, ferric oxide cannot be reduced to ferrous oxide, and thus Reactions (2) and (3) cannot be triggered.

Besides, quartz cannot react with aluminum oxide. That is to say, there is nearly no reaction in this system at temperatures below 610 K. At 610 K and beyond, the Gibbs free energy change of Reaction (2) is negative, clarifying that the reaction of ferrous oxide and aluminum oxide can occur. As we can see, the curve of Reaction (2) intersects the curve of Reaction (4) corresponding to the reaction of quartz and aluminum oxide at 1320 K, implying that aluminum oxide is more readily to react with ferrous oxide to form hercynite at 610–1320 K and that aluminum oxide prefers to reacting with quartz to form mullite at 1320–1700 K.

Considering the fact that silica may react with hercynite to produce mullite, the thermodynamic analysis of the reaction is further conducted. As shown in Fig. 2, tridymite could further react with hercynite to form mullite according to Reaction (5), if there is a portion of quartz transforming to tridymite over 1143 K [22], however, quartz could not react with hercynite. This can lead us to draw a conclusion that hercynite is thermodynamically stable at 610–1143 K and the presence of tridymite is unfavorable to the stability of hercynite in this system.

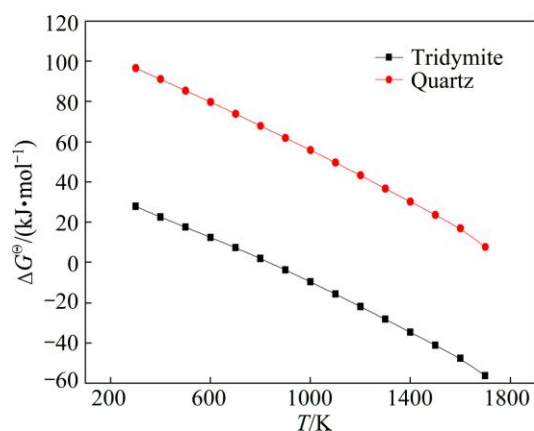
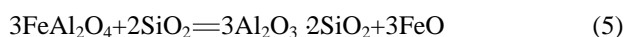


Fig. 2 Relationship between Gibbs free energy change of Reaction (5) and sintering temperature

3 Experimental

3.1 Materials

Al_2O_3 , Fe_2O_3 , SiO_2 and CaF_2 , purchased from China National Medicines Corporation Limited, are in analytical grade. Carbon used as the reductant is in medical grade and that used for maintaining reductive atmosphere is graphite powder. The raw material of kaolin purchased from Fujian Province, China, mainly consists of mica ($\text{KAl}_2\text{Si}_3\text{AlO}_{10}(\text{OH})_2$), kaolin ($\text{Al}_2\text{O}_3 \cdot 2\text{SiO}_2 \cdot 2\text{H}_2\text{O}$), quartz (SiO_2) and feldspar (KAlSi_3O_8 and $\text{NaAlSi}_3\text{O}_8$) by X-ray diffraction analysis as shown in Fig. 3, and contains 35% Al_2O_3 and 46% SiO_2 , according to the chemical component analysis.

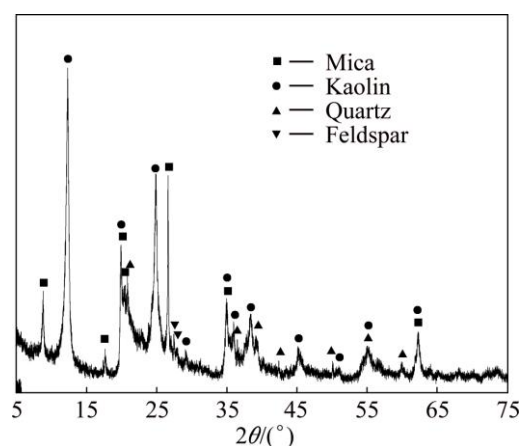


Fig. 3 XRD pattern of raw material of kaolin

3.2 Method

3.2.1 Raw meal preparation

All of the raw materials were milled to required granularity (less than 0.074 mm), and 50 g milled raw materials were then thoroughly mixed in stoichiometric proportions according to the studied reactions by using the DF-4 electromagnetic ore muller (Hangzhou Tongqi Instrument Company Limited, China) for at least twice with 2 min each time. It should be noted that the amount of carbon powder added as the reductant was 140% of the theoretical amount. Additionally, CaF_2 was added as the mineralizer and its dosage was 4% of the total mass of the raw meal.

3.2.2 Sintering process

5 g raw meal was placed into a 30 mL porcelain crucible covered by a lid with a layer of powdered carbon on it, and then the small porcelain crucible was put in a 100 mL corundum crucible with a layer of powdered carbon on the inner lining and the bottom. The corundum crucible was also covered by a lid in order to guarantee the reductive atmosphere during the sintering process. Subsequently, the corundum crucible was placed and heated in the muffle furnace at a preset temperature for certain residence time. The sintering temperature was in the range of 1027–1273 K with an interval of 100 K and the range of sintering time was 20–120 min with an interval of 20 min.

3.2.3 Phase analysis

The resulting products, namely clinkers, were cooled in the protective atmosphere. The clinkers obtained under different sintering conditions were detected by X-ray diffraction using the Bruker D8 (Bruker Company, Germany) with the scintillation counter of linear range of 2×10^6 cps. In addition, the Bruker D8 used an X-ray tube with a Cu anode as the primary X-ray beam source and its goniometer precision was 0.0001°.

4 Results and discussion

4.1 Reductive sintering in binary system $\text{Fe}_2\text{O}_3\text{-SiO}_2$

The powdered ferric oxide, silicon dioxide and carbon were mixed according to the molar ratio of 2:2:1.4. The XRD patterns of the clinkers obtained are shown in Figs. 4–6. It can be observed from Fig. 4 that no characteristic diffraction peak of ferrous silicate appears at sintering temperature of 1073 K for residence time of 20–120 min, showing that ferric oxide can hardly react with silicon dioxide in the form of quartz to form ferrous silicate (Reaction (3)) below 1073 K in the reductive atmosphere and further verifying the results in Fig. 1. And there are characteristic diffraction peaks of ferrous silicate in Figs. 5(b), (c) and Fig. 6, suggesting that ferric oxide starts to react with tridymite to form ferrous silicate at sintering temperature up to 1173 K for

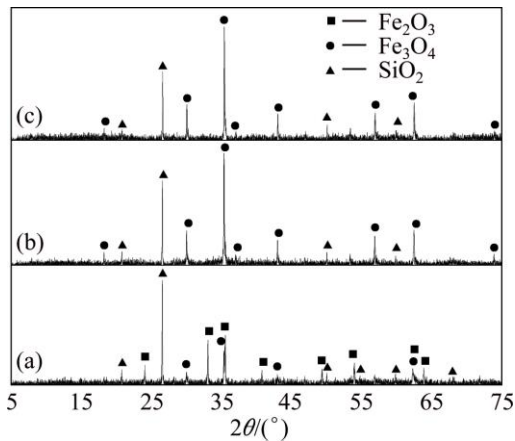


Fig. 4 XRD patterns of clinkers obtained from raw meal of Fe_2O_3 and SiO_2 by reductive sintering at 1073 K with $\text{Fe}_2\text{O}_3/\text{SiO}_2/\text{C}$ molar ratio of 2:2:1.4 for different residence time: (a) 20 min; (b) 60 min; (c) 120 min

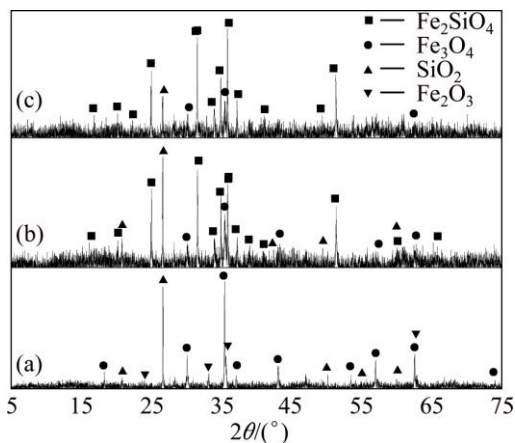


Fig. 5 XRD patterns of clinkers obtained from raw meal of Fe_2O_3 and SiO_2 by reductive sintering at 1173 K with $\text{Fe}_2\text{O}_3/\text{SiO}_2/\text{C}$ molar ratio of 2:2:1.4 for different residence time: (a) 20 min; (b) 60 min; (c) 120 min

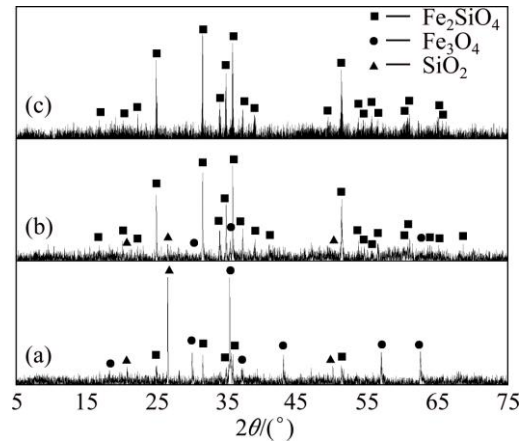


Fig. 6 XRD patterns of clinkers obtained from raw meal of Fe_2O_3 and SiO_2 by reductive sintering at 1273 K with $\text{Fe}_2\text{O}_3/\text{SiO}_2/\text{C}$ molar ratio of 2:2:1.4 for different residence time: (a) 20 min; (b) 60 min; (c) 120 min

60 min in the reductive atmosphere. But characteristic diffraction peaks of silica still exist in Figs. 5(b), (c) and Figs. 6(a), (b), meaning that it is hard to drive the reaction to completion with the limitation of sintering temperature and residence time. When the sintering temperature is 1273 K and the residence time is 120 min (Fig. 6(c)), only characteristic diffraction peaks of ferrous silicate exist, which shows that ferric oxide can react with silicon dioxide completely to form ferrous silicate in the reductive atmosphere under the sintering conditions. The experimental results are in good agreement with the previous thermodynamics.

4.2 Reductive sintering in binary system $\text{Fe}_2\text{O}_3\text{-Al}_2\text{O}_3$

The powdered ferric oxide, aluminum oxide and carbon were mixed at molar ratio of 2:4:1.4 and the XRD results of the clinkers obtained are presented in Figs. 7–9. At 1073 K for 20–120 min and at 1173 K for 20 min,

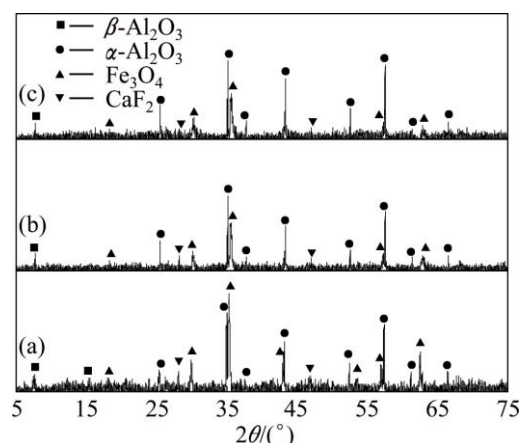


Fig. 7 XRD patterns of clinkers obtained from raw meal of Fe_2O_3 and Al_2O_3 by reductive sintering at 1073 K with $\text{Fe}_2\text{O}_3/\text{Al}_2\text{O}_3/\text{C}$ molar ratio of 2:4:1.4 for different residence time: (a) 20 min; (b) 60 min; (c) 120 min

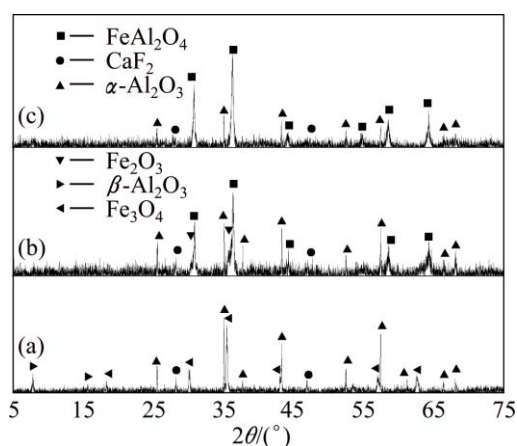


Fig. 8 XRD patterns of clinkers obtained from raw meal of Fe_2O_3 and Al_2O_3 by reductive sintering at 1173 K with $\text{Fe}_2\text{O}_3/\text{Al}_2\text{O}_3/\text{C}$ molar ratio of 2:4:1.4 for different residence time: (a) 20 min; (b) 60 min; (c) 120 min

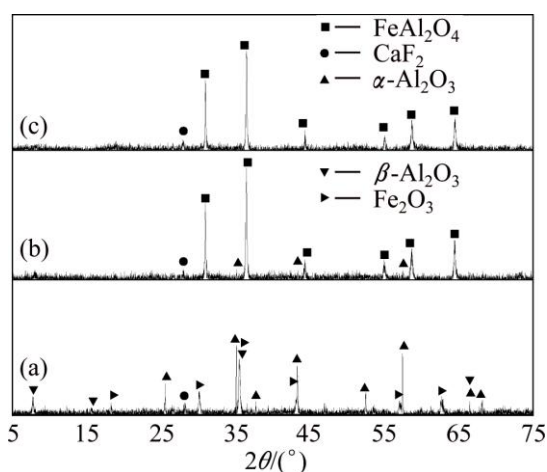


Fig. 9 XRD patterns of clinkers obtained from raw meal of Fe_2O_3 and Al_2O_3 by reductive sintering at 1273 K with $\text{Fe}_2\text{O}_3/\text{Al}_2\text{O}_3/\text{C}$ molar ratio of 2:4:1.4 for different residence time: (a) 20 min; (b) 60 min; (c) 120 min

the hercynite peak is not found in Fig. 7 and Fig. 8(a), demonstrating that, in the reductive atmosphere, ferric oxide can hardly react with aluminum oxide to form hercynite (Reaction (2)) under these conditions possibly due to too low reaction rate in kinetics. The hercynite peak in Fig. 8(b) shows that ferric oxide begins to react with aluminum oxide at sintering temperature up to 1173 K for 60 min in the reductive atmosphere; however, the $\alpha\text{-Al}_2\text{O}_3$ peaks shown in Fig. 8(c) imply that the reaction is unable to be completely finished in 120 min due to the restriction of sintering temperature. As we can see in Fig. 9, in the reductive atmosphere, when the sintering temperature reaches 1273 K, ferric oxide is hard to react with aluminum oxide for 20 min and it can thoroughly react with aluminum oxide to form hercynite for 120 min.

4.3 Reductive sintering in ternary system $\text{Fe}_2\text{O}_3\text{-SiO}_2\text{-Al}_2\text{O}_3$

The powdered ferric oxide, silicon dioxide, aluminum oxide and carbon were proportionally mixed at the molar ratio of 2:2:4:1.4. The XRD results of sintering products are shown in Figs. 10–12. It can be found that there are nearly no reactions among ferric oxide, aluminum oxide and silicon dioxide in the reductive atmosphere both at 1073 K for 20–120 min and at 1173 K for 20 min (Fig. 10 and Fig. 11(a)). For the sintering temperature up to 1173 K, ferric oxide reacts with aluminum oxide to form hercynite (Reaction (2)), but it does not react with silicon dioxide to form ferrous silicate (Reaction (3)) in the reductive atmosphere for 60–120 min (Figs. 11(b), (c)). When sintering temperature increases to 1273 K, all the ferric oxides react only with aluminum oxide thoroughly to form hercynite in the reductive atmosphere for 120 min,

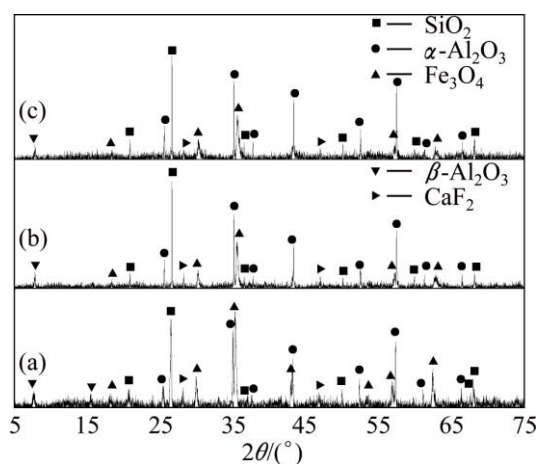


Fig. 10 XRD patterns of clinkers obtained from raw meal of Fe_2O_3 , SiO_2 and Al_2O_3 by reductive sintering at 1073 K with $\text{Fe}_2\text{O}_3/\text{SiO}_2/\text{Al}_2\text{O}_3/\text{C}$ molar ratio of 2:2:4:1.4 for different residence time: (a) 20 min; (b) 60 min; (c) 120 min

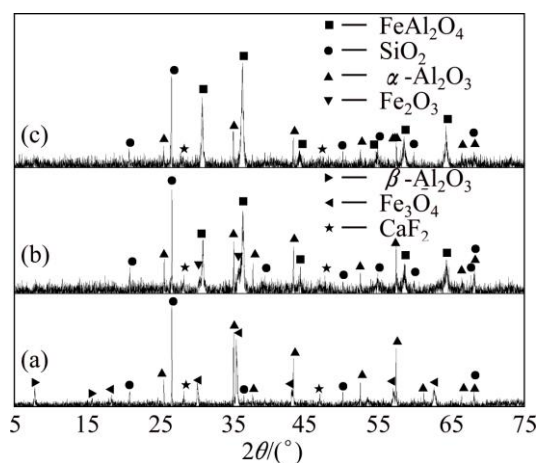


Fig. 11 XRD patterns of clinkers obtained from raw meal of Fe_2O_3 , SiO_2 and Al_2O_3 by reductive sintering at 1173 K with $\text{Fe}_2\text{O}_3/\text{SiO}_2/\text{Al}_2\text{O}_3/\text{C}$ molar ratio of 2:2:4:1.4 for different residence time: (a) 20 min; (b) 60 min; (c) 120 min

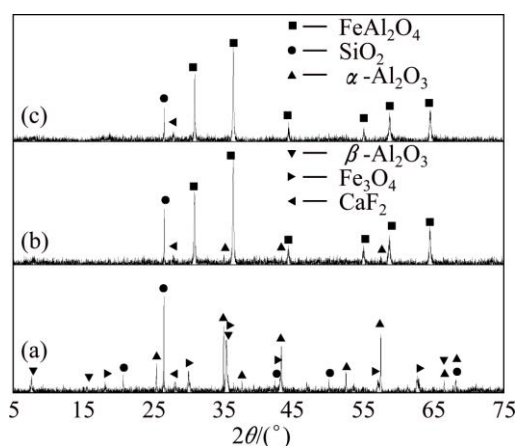


Fig. 12 XRD patterns of clinkers obtained from raw meal of Fe_2O_3 , SiO_2 and Al_2O_3 by reductive sintering at 1273 K with $\text{Fe}_2\text{O}_3/\text{SiO}_2/\text{Al}_2\text{O}_3/\text{C}$ molar ratio of 2:2:4:1.4 for different residence time: (a) 20 min; (b) 60 min; (c) 120 min

in other words, silicon dioxide is not able to react with ferric oxide to form ferrous silicate due to the lack of ferric oxide (Fig. 12), being consistent with the thermodynamic analyses in Section 2.

In order to reveal what the outcome would be if there is enough ferric oxide in the system, the powdered ferric oxide, silicon dioxide, aluminum oxide and carbon were mixed according to the molar ratio of 2:2:1:1.4 and the raw meal was sintered at 1273 K for 120 min. As seen in Fig. 13, if ferric oxide is enough, the clinker obtained contains both hercynite and ferrous silicate, further proving that Reaction (3) of ferrous oxide and silicon dioxide takes place only when there is surplus ferric oxide after hercynite formation in the reductive sintering system $\text{Fe}_2\text{O}_3\text{-SiO}_2\text{-Al}_2\text{O}_3$.

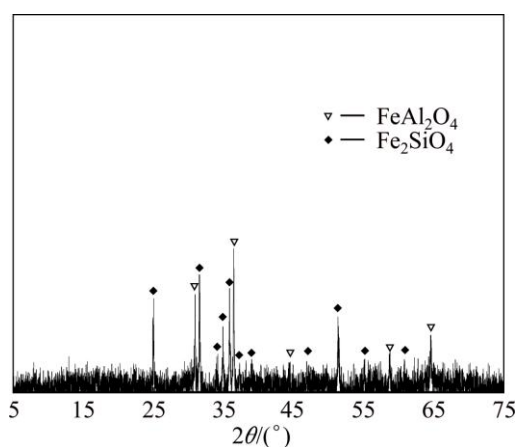


Fig. 13 XRD pattern of clinkers obtained from raw meal of Fe_2O_3 , SiO_2 and Al_2O_3 by reductive sintering at 1273 K for 120 min with $\text{Fe}_2\text{O}_3/\text{SiO}_2/\text{Al}_2\text{O}_3/\text{C}$ molar ratio of 2:2:1:1.4

To determine whether the experimental results based on pure substances are adaptable to aluminosilicate

minerals and study what would happen at higher sintering temperatures, kaolin, ferric oxide and carbon were employed as raw materials to further explore the reaction behavior of ferric oxide. Kaolin and ferric oxide were mixed with the mass ratio of 3.64:1 in order to ensure that the molar ratio of aluminum oxide, silicon dioxide and iron oxide in raw meal was the same as that in Figs. 10–12. The range of sintering temperature was 873–1673 K and residence time was 2 h. We can see from Fig. 14 that Al/Si-bearing compounds in the kaolin can hardly react with ferrous oxide below 1073 K in the reductive atmosphere. At 1073–1273 K, the hercynite peak can be observed and the diffraction intensities increase with the increase of temperature, showing that Al/Si compounds in the kaolin can react with FeO generated by the reductive reaction of Fe_2O_3 with C to form hercynite (Reaction (2)). When the temperature reaches 1473 K, the intensities of hercynite peaks decrease with mullite peaks appearing, and the hercynite peaks disappear while the mullite peaks increase in intensity at 1573 and 1673 K. This suggests that hercynite generated firstly can react with silicon dioxide to form mullite (Reaction (5)) at temperature above 1473 K, being in consistence with the previous theoretic analysis.

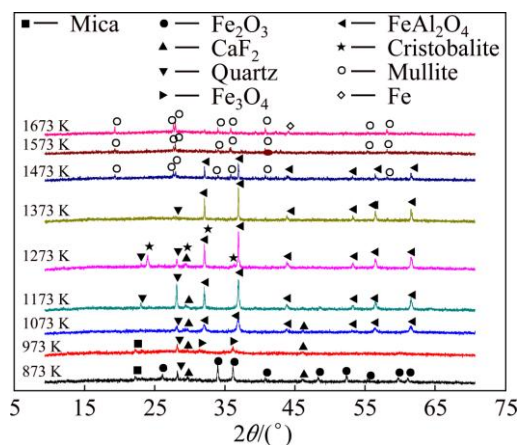


Fig. 14 XRD patterns of clinkers obtained from raw meal of kaolin and Fe_2O_3 by reductive sintering at different temperatures for 120 min

5 Conclusions

1) Thermodynamic analyses indicate that, in the reductive sintering system $\text{Fe}_2\text{O}_3\text{-SiO}_2\text{-Al}_2\text{O}_3$, the stable phase is hercynite at 610–1143 K and it will further react with tridynite to form mullite over 1143 K.

2) Reductive sintering experimental results show that ferric oxide can react with silicon dioxide and aluminum oxide to form ferrous silicate and hercynite respectively at 1273 K for 120 min.

3) In the ternary reductive sintering system

$\text{Fe}_2\text{O}_3\text{-SiO}_2\text{-Al}_2\text{O}_3$, ferrous oxide formed by the reductive reaction of ferric oxide with carbon, preferentially reacts with aluminum oxide to form hercynite, while the reaction of the ferrous oxide with silicon dioxide occurs only when there is surplus ferrous oxide after the exhaustion of aluminum oxide. Moreover, the hercynite generated firstly would further react with silicon dioxide to ultimately form mullite at higher sintering temperatures.

4) Aluminum compounds in aluminosilicate can be stabilized in the form of hercynite under the following conditions: sintering temperature 1273–1373 K, residence time 60–120 min, $\text{Fe}_2\text{O}_3/\text{Al}_2\text{O}_3$ molar ratio 2:1, and proper reductive atmosphere.

References

- [1] GAO Shu-ling, LI Xiao-an, WEI De-zhou, FANG Ping, JIA Chun-yun, LIU Wen-gang, HAN Cong. Beneficiation of low-grade diaspore bauxite with hydrocyclone[J]. Transactions of Nonferrous Metals Society of China, 2008, 18(2): 444–448.
- [2] WU Rong-qing. Present situation and development strategy of bauxite [J]. China Metal Bulletin, 2013, 39: 28–33. (in Chinese)
- [3] ZHANG He-lun, HE Jing-hua, ZHANG Ying. Present situation and development countermeasure of alumina industry in China [J]. Light Metals, 2006(2): 3–7. (in Chinese)
- [4] NAN Xiang-li, ZHANG Ting-an, LIU Yan, DOU Zhi-he. The comprehensive utilization of red mud analysis in our country [J]. The Chinese Journal of Process Engineering, 2010, 10(S1): s264–s269.
- [5] YANG Quan-cheng, MA Shu-hua, XIE Hua, ZHEN Shi-li. Research progress of extracting alumina from high-aluminum fly ash [J]. Multipurpose Utilization of Mineral Resources, 2012(3): 4–6. (in Chinese)
- [6] ZHONG Li, ZHANG Yi-fei, ZHANG Yi. Extraction of alumina and sodium oxide from red mud by a mild hydro-chemical process [J]. Journal of Hazardous Materials, 2009, 172(2): 1629–1634.
- [7] MISHRA B, STALEY A, KIRKAPTRICK D. Recovery of value-added products from red mud [J]. Minerals & Metallurgical Processing, 2002, 19(2): 87–94.
- [8] ERCAG E, APAK R. Furnace smelting and extractive metallurgy of red mud: Recovery of TiO_2 , Al_2O_3 and pig iron [J]. Journal of Chemical Technology & Biotechnology, 1997, 70(3): 241–246.
- [9] SNARS K, GILKERS R J. Evaluation of bauxite residues (red muds) of different origins for environmental applications [J]. Applied Clay Science, 2009, 46(1): 13–20.
- [10] FOIS E, LALLAI A, MURA G. Sulfur dioxide absorption in a bubbling reactor with suspensions of Bayer red mud [J]. Industrial & Engineering Chemistry Research, 2007, 46(21): 6770–6776.
- [11] LIU Y J, NAIDU R, MING H. Red mud as an amendment for pollutants in solid and liquid phases [J]. Geoderma, 2011, 163(1): 1–12.
- [12] GUPTA V K, GUPTA M, SHAMA S. Process development for the removal of lead and chromium from aqueous solutions using red mud—An aluminum industry waste [J]. Water Research, 2001, 35(5): 1125–1134.
- [13] BAI Guang-hui, TENG Wei, WANG Xiang-gang, QIN Jin-guo, XU Peng, LI Peng-cheng. Alkali desilicated coal fly ash as substitute of bauxite in lime-soda sintering process for aluminum production [J]. Transactions of Nonferrous Metals Society of China, 2010, 20(S1): s169–s175.
- [14] LI Xiao-bin, ZHANG Zhi-qiang, LIU Wei, LIU Gui-hua, PENG Zhi-hong, ZHOU Qiu-sheng. Reaction behavior of Al_2O_3 and Fe_2O_3 in $\text{Na}_2\text{O-Al}_2\text{O}_3\text{-Fe}_2\text{O}_3$ systems during sintering [J]. The Chinese Journal of Process Engineering, 2009, 9(5): 877–881.
- [15] KELLEY K K. The specific heats at low temperatures of ferrous silicate, manganous silicate and zirconium silicate [J]. Journal of the American Chemical Society, 1941, 63(10): 2750–2752.
- [16] ZHANG Jun-bo, ZHANG Gang, XIAO Guo-qing. Preparation of hercynite [J]. Bulletin of the Chinese Ceramic Society, 2007, 26(5): 1003–1006.
- [17] SCHAIRER J F. The system $\text{CaO-FeO-Al}_2\text{O}_3\text{-SiO}_2$: I. Results of quenching experiments on five joins [J]. Journal of the American Chemical Society, 1942, 25(10): 241–274.
- [18] LI Hai-bo, LIU Mei, XU Ying, XU Shi-zhong, YU Wen-xue. Structure and magnetic properties of $\text{Fe/Al}_2\text{O}_3$ nanocomposites [J]. Journal of Jilin University: Engineering and Technology Edition, 2007, 37(4): 1073–1083. (in Chinese)
- [19] BOTTA P M, BERCOFF P G, AGLIETTI E F, BERTORELLO H R, PORTO L O PEZ J M. Magnetic and structural study of mechanochemical reactions in the $\text{Al-Fe}_3\text{O}_4$ system [J]. Journal of Materials Science, 2002, 37(12): 2563–2568.
- [20] YE Da-lun, HU Jian-hua. Practical inorganic substances thermodynamic data manual [M]. Beijing: Metallurgical Industry Press, 2002. (in Chinese)
- [21] MEI Xian-gong, SUN Zong-yi, CHEN Jin. Thermodynamic analysis of the solid reactions in the direct reduction process of high-iron red mud by coal [J]. Light Metals, 1994(7): 8–12. (in Chinese)
- [22] LIU Li, MA Hong-xiang, LÜ Jian-ming. Comparative study of NaCl and NaOH on the effect of crystal shape conversion [J]. Guangzhou Chemical Industry, 2013, 41(19): 49–51. (in Chinese)

$\text{Fe}_2\text{O}_3\text{-SiO}_2\text{-Al}_2\text{O}_3$ 系还原烧结过程中 Fe_2O_3 的反应行为

周秋生, 李 闯, 李小斌, 彭志宏, 刘桂华, 齐天贵

中南大学 冶金与环境学院, 长沙 410083

摘 要: 以纯化合物和高岭土为原料, 研究 $\text{Fe}_2\text{O}_3\text{-SiO}_2\text{-Al}_2\text{O}_3$ 三元系还原烧结过程中 Fe_2O_3 的反应行为。热力学计算分析和还原烧结实验结果表明, 在还原性碳气氛中, 1173 K 下 Fe_2O_3 被还原后得到的 FeO 能分别与 SiO_2 和 Al_2O_3 反应生成硅酸亚铁和铝酸亚铁。对于 $\text{Fe}_2\text{O}_3\text{-SiO}_2\text{-Al}_2\text{O}_3$ 三元系, 在还原性气氛条件下, Fe_2O_3 还原后形成的 FeO 将优先与 Al_2O_3 反应形成铝酸亚铁, 只有当体系中 Al_2O_3 反应完全后还存在过量的 FeO 时, SiO_2 才能与 FeO 反应形成硅酸亚铁。当烧结温度继续升高到 1473 K 时, 三元系中形成的铝酸亚铁将进一步与体系中的 SiO_2 反应生成莫来石和 FeO 。研究结果有望为氧化铝生产过程中低 A/S 比含铁原料的铝硅分离提供新的思路。

关键词: 还原烧结; 氧化铁; 硅酸亚铁; 铁尖晶石; 莫来石; 高岭土

(Edited by Wei-ping CHEN)